



Published in final edited form as:

Science. 2019 January 18; 363(6424): 270–275. doi:10.1126/science.aav3421.

## Concise total syntheses of (–)-Jorunnamycin A and (–)-Jorumycin enabled by asymmetric catalysis

Eric R. Welin<sup>1</sup>, Aurapat Ngamnithiporn<sup>1</sup>, Max Klatte<sup>1</sup>, Guillaume Lapointe<sup>1</sup>, Gerit M. Pototschnig<sup>1</sup>, Martina S. J. McDermott<sup>2</sup>, Dylan Conklin<sup>2</sup>, Christopher D. Gilmore<sup>1</sup>, Pamela M. Tadross<sup>1</sup>, Christopher K. Haley<sup>1</sup>, Kenji Negoro<sup>1</sup>, Emil Glibstrup<sup>1</sup>, Christian U. Grünanger<sup>1</sup>, Kevin M. Allan<sup>1</sup>, Scott C. Virgil<sup>1</sup>, Dennis J. Slamon<sup>2</sup>, Brian M. Stoltz<sup>1</sup>

<sup>1</sup>The Warren and Katharine Schlinger Laboratory of Chemistry and Chemical Engineering, California Institute of Technology, Pasadena, California 91125, United States.

<sup>2</sup>Division of Hematology/Oncology, Department of Medicine, Geffen School of Medicine at UCLA, Los Angeles, California.

### Abstract

The bis-tetrahydroisoquinoline (bis-THIQ) natural products have been studied intensively over the past four decades for their exceptionally potent anticancer activity, in addition to strong gram-positive and -negative antibiotic character. Synthetic strategies toward these complex polycyclic compounds have relied heavily on electrophilic aromatic chemistry, such as the Pictet-Spengler reaction, that mimics their biosynthetic pathways. Herein we report an approach to two bis-THIQ natural products, jorunnamycin A and jorumycin, that instead harnesses the power of modern transition-metal catalysis for the three major bond-forming events and proceeds with high efficiency (15 and 16 steps, respectively). By breaking from biomimicry, this strategy allows for the preparation of a more diverse set of non-natural analogs.

The bis-tetrahydroisoquinoline (bis-THIQ) natural products have been studied intensively by chemists and biologists alike during the 40+ years since their initial discovery due to their intriguing chemical structures, potent biological activities, and unique mechanisms of action (1, 2). Jorumycin (**1**, Fig. 1) and its congeners ecteinascidin 743 (Et 743, **2**) and jorunnamycin A (**3**) possess a pentacyclic carbon skeleton, highly oxygenated ring termini, and a central pro-iminium ion (manifested either as a carbinolamine or an  $\alpha$ -aminonitrile motif). This latter functionality serves as an alkylating agent *in vivo*, resulting in covalent

**Author Contributions:** B.M.S. conceived and directed the project. E.R.W., C.D.G., P.M.T., K.M.A., and B.M.S. conceptualized and designed the synthetic strategy. E.R.W., A.N., M.K., G.L., G.M.P., C.D.G., P.M.T., C.K.H., K.N., E.G., and C.U.G. designed, performed, and analyzed the synthetic chemistry experiments. E.R.W., A.N., and G.M.P. designed and synthesized bis-THIQ analogs **31–34**. D.J.S., M.S.J.M. and D.C. designed, performed, and analyzed biological activity experiments. S.C.V. assisted with experimental design and purification and obtained x-ray quality crystals of bis-THIQ **27**. E.R.W., A.N., G.M.P., and B.M.S. prepared the manuscript. D.J.S. and B.M.S. acquired funding for the project.

**Competing Interests:** B.M.S. has received financial support unrelated to the current science from 1200 Pharma, LLC, Novartis, Holoclara, and Amgen. B.M.S. is a co-founder of 1200 Pharma, LLC. The California Institute of Technology holds a patent on methods for preparing bis-tetrahydroisoquinoline-containing compounds, on which E.R.W., A.N., M.K., G.L., G.M.P., C.D.G., P.M.T., C.K.H., K.N., C.U.G., K.M.A., S.C.V., and B.M.S. are named as inventors.

**Data and materials availability:** Crystallographic parameters for compound **27** are available free of charge from the Cambridge Crystallographic Data Centre under CCDC 1875455. Data are available in the supplementary materials. The molecular characterization of the cell lines used in this Report has been deposited in the GEO public database (GEO:GSE18496).

modification of DNA in a process that ultimately leads to cell death (3). The promise of these natural products as anticancer agents has been realized in the case of Et 743 (Yondelis<sup>®</sup>, trabectedin), which has been approved in the US, Europe, and elsewhere for the treatment of a variety of drug-resistant and unresectable soft-tissue sarcomas and ovarian cancer (3). Unfortunately, although **2** is available from nature, isolation of one gram of the drug would require more than one ton of biological material. For this reason, the successful application of **2** as an antitumor agent has necessitated its large-scale chemical synthesis, a 21-step process that begins with cyanosafracin A, a fermentable and fully functionalized bis-THIQ natural product (4). This has restricted medicinal chemistry endeavors via this route to the production of only compounds with a high degree of similarity to the natural products themselves.

Intriguingly, although **1** and **3** possess quinone rings, these moieties are rapidly reduced in cells to their hydroquinone oxidation states, more closely resembling those of **2** (5). These highly electron-rich functional groups are key components in the biosynthetic pathways of the bis-THIQ's, which are forged by the action of Pictet–Spenglerase enzymes (6, 7). Previously reported chemical syntheses of bis-THIQ natural products feature elegant and creative application of electrophilic aromatic substitution (EAS) chemistry for the construction of one or more of the THIQ motifs. Though highly enabling, this approach has also limited the synthesis of non-natural analogs to highly natural product-like derivatives. As a key example, despite the scores of analogs produced over the past few decades (8–11), the majority of the derivatives focus on substitution of the heteroatom moiety appended to the B-ring (cf. structure **4**, Fig. 1), and only a select few possess significant structural and substitutional variation around the aromatic or quinone A- and E-rings (8–11). Furthermore, derivatives possessing electron-withdrawing groups on these rings are inaccessible using biomimetic approaches, as these would inhibit the EAS chemistry used to construct the THIQs. This latter point is significant, as studies have indicated that the smaller bis-THIQ natural products such as **1** and **3** are more susceptible to metabolic degradation than Et 743 and other larger bis-THIQs (12, 13), and the installation of electron-withdrawing groups is a commonly employed strategy to improve a drug molecule's metabolic stability (14).

Jorumycin has been the target of four total syntheses (15–18) and two semisyntheses (19, 20) since its isolation in 2000 (21), and jorunnamycin A has frequently been prepared en route. Jorumycin displays IC<sub>50</sub>'s of 0.24 nM vs. A549 lung cancer, 0.49 nM vs. DU145 prostate cancer, and 0.57 nM vs. HCT116 colon cancer (17, 19, 21), among others, thus offering immense therapeutic potential. Furthermore, jorumycin and jorunnamycin A are appealing targets for further synthetic elaboration: the oxygen substitution appended to the B-ring (cf. structure **4**, X = OH, Fig. 1) could allow rapid diversification to the ecteinascidin, saframycin, safracin, and renieramycin scaffolds (1). To overcome the limitations of the current state of the art with respect to analog diversity, we sought an alternative, non-biomimetic route to these natural products.

Specifically, we envisioned the retrosynthetic strategy shown in Fig. 2A. We posited that a late stage oxygenation event to provide jorumycin (**1**) would greatly simplify the construction of the precursor, pentacycle **6**. We then considered disconnection of the central C-ring (cf. Fig. 1) through cleavage of the lactam moiety in **6**, providing bis-THIQ

compound **7**. Critically, bis-THIQ structure **7** was recognized as a potential product of an enantioselective hydrogenation of bis-isoquinoline **8**. The central biaryl bond of **8** could be formed through a C–H cross-coupling reaction, leading to isoquinoline monomers **9** and **10**, thus greatly simplifying the synthetic challenge. As a key advantage, isoquinolines **9** and **10** could be prepared through the application of any known method, not limited only to those requiring highly electron-rich and  $\pi$ -nucleophilic species. Crucially, this approach would allow access to the natural products themselves, as well as derivatives featuring substantial structural and/or electronic variation.

As shown in Fig. 2B, we initiated our synthetic studies with the Sonogashira coupling of aryl bromide **11** (available in two steps from 3,5-dimethoxybenzaldehyde, see Supplementary Materials) with *tert*-butyldimethylsilyl propargyl ether (**12**); simply adding solid hydroxylamine hydrochloride to the reaction mixture after the coupling provided oxime-bearing alkyne **13** in 99% yield. Catalytic silver(I) triflate activated the alkyne toward nucleophilic attack by the oxime, directly generating isoquinoline *N*-oxide **9** in 77% yield on up to a 12-gram scale (22). Next, we began our synthesis of isoquinoline triflate **10** by using aryne-based methodology developed in our laboratories (23). Silyl aryl triflate **14** (available in 3 steps from 2,3-dimethoxytoluene, see Supplementary Materials) was treated with cesium fluoride to generate the corresponding aryne intermediate *in situ* (not shown), which underwent aryne acylalkylation with *in situ* condensation to provide 3-hydroxy-isoquinoline **16** in 45% yield. Reaction with trifluoromethanesulfonic anhydride provided electrophilic coupling partner **10** in 94% yield.

With working routes to both isoquinoline monomers in hand, we turned our attention to the palladium-catalyzed cross-coupling reaction which would be used to construct the carbon skeleton of jorumycin. We were pleased to find that isoquinolines **9** and **10** were efficiently coupled under modified conditions developed by Fagnou and co-workers to provide bis-isoquinoline **18** in 94% yield on a 7-gram scale (24). This large-scale application of C–H activation likely proceeds through a transition state similar to **17** and allows for the direct construction of **18** without the need for prefuctionalization (25). The excess of *N*-oxide **9** required to achieve maximum levels of efficiency appears to be only a kinetic factor, as all excess **9** was recovered after the reaction.

At this stage, we sought to install the level of oxidation necessary to initiate our hydrogenation studies (Fig. 2C). Specifically, this required selective oxidation of the nitrogen-adjacent methyl and methylene groups on the B- and D-rings, respectively. We attempted a double-Boekelheide rearrangement to transpose the *N*-oxidation to both *C*-positions simultaneously, effecting formal C–H oxidation reactions (26). Unfortunately, after oxidation to intermediate bis-*N*-oxide **19**, only the B-ring azine underwent rearrangement. Despite this setback, we found that it was possible to parlay this reactivity into a one-pot protocol by adding acetic anhydride upon complete oxidation, providing differentially protected diol **20** in 62% yield. N–O bond cleavage and oxyl-mediated oxidation provided bis- isoquinoline **8** in two additional steps. To date, we have produced more than 5 grams of bisisoquinoline **8**.

With a scaleable route to isoquinoline **8** in hand, we turned our attention to the key hydrogenation event. If successful, this strategic disconnection would add four molar equivalents of hydrogen, create four new stereocenters, and form the central C-ring lactam. Although the enantioselective hydrogenation of nitrogen-based heterocycles is a well-studied reaction, isoquinolines are possibly the most challenging and least investigated substrates (27). To our knowledge only four reports existed prior to our studies that describe asymmetric isoquinoline hydrogenation, and only one appears to tolerate 1,3-disubstitution patterns (28-31).

We nonetheless noted that metal-catalyzed imine and carbonyl reduction is a comparatively successful and well-studied transformation (32, 33). We were drawn to the iridium catalyst developed by scientists at Ciba-Geigy (now Syngenta) for asymmetric ether-directed imine reduction in the preparation of Metolachlor (34). Considering the positioning of the hydroxymethyl group appended to the B-ring of **8** and the electronic similarity of the adjacent C1–N  $\pi$ -bond to that of an imine, we posited that a similar catalytic system might be used to direct the initial reduction to this position (Fig 3). Furthermore, the chelation mode was attractive as a scaffolding element to enable enantioselective *S*i**-face reduction. In keeping with previous observations (28-31), we anticipated that full B-ring reduction would provide *cis*-mono-THIQ **22** as the major product. We believed that **22** would then act as a tridentate ligand for a metal ion (although not necessarily the catalytically active species), and the three-dimensional coordination environment of metal-bound **22**•**M** would direct D-ring hydrogenation from the same face. Finally, the all-*syn* nature of **7** places the ester moiety in proximity to B-ring secondary amine, and we expected lactamization to be rapid. If successful, this self-reinforcing diastereoselectivity model would allow for control over the four new stereocenters and produce the bis-THIQ core in a single step.

Upon beginning our enantioselective hydrogenation studies, we found that we could identify trace amounts of conversion to mono-THIQ product **22** by using the catalyst mixture developed at Ciba-Geigy (34), thus confirming the accelerating effects of the pendent hydroxy directing group. Under these general conditions, we then performed a broad evaluation of more than 60 chiral ligands commonly used in enantioselective catalysis protocols (see Supplementary Materials). From this survey, we identified three ligands that provided **22** in at least 80% enantiomeric excess (ee) and with uniformly excellent diastereoselectivity (all >20:1 diastereomeric ratio, dr): (*S*)-(CF<sub>3</sub>)-*t*-BuPHOX (**23**, Entry 2, 22% yield, –82% ee), (*S,S*)-Et-FerroTANE (**24**, Entry 3, 26% yield, –87% ee), and (*S,R<sub>p</sub>*)-Xyliphos (**25**, Entry 4, 30% yield, 80% ee). After evaluating these ligand classes further, we identified (*S,R<sub>p</sub>*)-BTfM-Xyliphos (**26**) (35) as a strongly activating ligand that provided mono-THIQ **22** in 83% yield, >20:1 dr, and in a remarkable 94% ee (Entry 5). Moreover, we were elated to find that ligand **26** formed a catalyst that provided pentacycle **6** as a single diastereomer in 10% yield. Further evaluation of the reaction parameters revealed that increasing temperature provided higher levels of reactivity, albeit at the expense of enantioselectivity (Entry 6, 31% yield of **22**, 87% ee, 43% yield of **6**). The best results were achieved by performing the reaction at 60 °C for 18 hours and then increasing the temperature to 80 °C for 24 hours. Under these conditions, **6** was isolated in 59% yield with >20:1 dr and 88% ee (Entry 7) (36). In the end, doubling the catalyst loading allowed us to

isolate **6** in 83% yield, also with >20:1 dr and 88% ee (Entry 8) on greater than 1 mmol scale. bis-THIQ **6** could be easily accessed in enantiopure form (>99% ee by HPLC) by crystallization from a slowly evaporating acetonitrile solution, and we were able to confirm the relative and absolute stereochemistry by obtaining an x-ray crystal structure on corresponding 4-bromophenyl sulfonamide **27**. Within the context of this synthesis, the relatively high catalyst loading (20 mol % Ir) is mitigated by the substantial structural complexity generated in this single transformation.

At this stage, we were poised to investigate the third and final key disconnection from our retrosynthetic analysis, namely, latestage C–H oxidation of the arenes (Fig. 4). To set up this chemistry the piperazinone N–H of **6** was methylated under reductive amination conditions in quantitative yield. Despite numerous attempts to effect catalytic C–H oxidation on this advanced intermediate, we found that a two-step procedure was necessary instead. We were able to chlorinate both of the remaining aromatic positions, providing bis-THIQ **28** in 68% yield. From here, we once again turned to catalysis, this time for the oxygenation of aryl halides. After extensive investigation, we found that Stradiotto and coworkers' recently developed protocol for the hydroxylation of aryl halides was uniquely effective (37). Further optimization revealed that the combination of adamantyl BippyPhos ligand with Buchwald's cyclometalated palladium(II) dimer was ideal (38), providing dihydroxylated bis-THIQ **29** in 46% yield, an impressive result for such a challenging coupling reaction on a sterically large, electron-rich, and Lewis-basic substrate in the final stages of the synthesis. Partial lactam reduction with cyanide trapping proceeded in 50% yield, and oxidation of the phenols provided jorunnamycin A (**3**) in only 15 linear steps. We isolated hemiacetal **30** in 33% yield, which was surprising given the generally low stability of acyclic hemiacetals. Finally, we developed conditions for the conversion of jorunnamycin A into jorumycin in a single step, providing **1** in 68% yield in 16 linear steps (1). Jorunnamycin A (**3**) and jorumycin (**1**) are produced in 0.24% and 0.17% yield, respectively, from commercially available materials, but key bis-THIQ **6**, the branching point for derivative synthesis, is accessed over 10 steps in 5.0% overall yield on greater than 500 mg scale. These efforts are similar to Zhu and coworkers' elegant synthesis of jorumycin with regard to brevity (16).

Central to the anticancer activity of the bis-THIQ natural products is the capacity to alkylate DNA upon loss of water or cyanide from the central carbinolamine or  $\alpha$ -cyanoamine, respectively (39). After alkylation, compelling evidence suggests formation of reactive oxygen species (5) or DNA-protein cross-links (8, 40) leads to cell-cycle arrest or cell death. We therefore synthesized analogs **31–34**, which feature the non-oxygenated framework as well as all permutations of partial and full oxygenation. The activity of this series would allow us to determine the relative importance of the location and degree of oxygenation on the A- and E-rings, the structure-activity relationships of which have not previously been explored.

With the backdrop that preclinical efficacy studies are complex and demanding, we conducted very preliminary studies to probe the relative cytotoxicity of synthetic analogues **31–34** and established that modifying one site on the scaffold greatly diminishes cytotoxicity, whereas other modifications conserved cytotoxicity. The cytostatic and cytotoxic properties of **31–34** were determined using long-term, growth-maximizing assay

conditions against 29 cancer cell lines known to be responsive in vitro to other general cytotoxics (Fig. 5, see Supplementary Materials) (41, 42). Cells were routinely assessed for mycoplasma contamination using a multiplex PCR method and STR profiling for cell-line authentication. This methodology differs markedly from the standard 72-hour, luminescence-based cytotoxicity assays employed most commonly for in vitro quantification of drug response. This approach was chosen as it is specifically well suited to determine the activity of compounds wherein anti-proliferative effects occur over a longer time period than standard cytotoxic agents. Perhaps not surprisingly, removal of both phenolic oxygens resulted in a complete loss in activity (i.e., **31**, all IC<sub>50</sub>'s > 1  $\mu$ M), while fully oxygenated bis-THIQ **34** showed cytotoxicity. The most notable results were provided by **32** and **33**, which possess A- and E-ring monohydroxylation, respectively. While compound **32**, which is devoid of E-ring oxygenation, showed diminished activity, we were surprised to find that compound **33** featuring only E-ring oxygenation maintained a similar activity profile to fully oxygenated **34** (see Supplementary Materials). At the moment, we believe these data to be the result of general cytotoxicity, as opposed to cancer cell-specific activity. As a reference, three out of four previously known anticancer agents that function through general cytotoxicity showed similar levels of activity in our model. While more sophisticated studies are necessary to determine actual efficacy, the ability to delete one oxygen atom and retain activity is both intriguing and unexpected.

The use of catalysis, rather than native reactivity, is a key advantage to our synthesis, allowing us to expedite access to both the natural products themselves, and also biologically relevant derivatives.

## Supplementary Material

Refer to Web version on PubMed Central for supplementary material.

## Acknowledgments.

The authors thank Stig H. Christensen for experimental assistance and M. Takase and L. Henling for assistance with x-ray structure determination.

**Funding:** Research reported in this publication was supported by the NIH National Institute of General Medical Sciences (R01 127972), the Margaret E. Early Medical Research Trust, the NSF under the CCI Center for Selective C–H Functionalization (CHE-1205646), the Teva Pharmaceuticals Marc A. Goshko Memorial Grant Program, and the California Institute of Technology RI2 Program. E.R.W. was supported by a Postdoctoral Fellowship, PF-16-011-01-CDD, from the American Cancer Society. A.N. was supported by the Royal Thai Government Scholarship program. M.K. was supported by a postdoctoral fellowship from the German Academic Exchange Service. G.L. was supported by the Swiss National Science Foundation. G.M.P. was supported by an Erwin Schrodinger Fellowship, J 3893–N34, from the Austrian Science Fund (FWF). P.M.T. was supported by a graduate fellowship from the California HIV/AIDS Research Program. E.G. was supported by Knud Højgaards Fond and Oticon Fonden. C.U.G. was supported by a Feodor Lynen Research Fellowship from the Alexander von Humboldt Foundation.

## References

1. Chrzanowska M, Grajewska A, Rozwadowska MD, Chem. Rev 116, 12369–12465 (2016). [PubMed: 27680197]
2. Newman DJ, Cragg GM, J. Nat. Prod 79, 629–661 (2016). [PubMed: 26852623]
3. Cuevas C, Francesch A, Nat. Prod. Rep 26, 322–337 (2009). [PubMed: 19240944]



4. Cuevas C, et al., *Org. Lett* 2, 2545–2548 (2000). [PubMed: 10956543]
5. Lown JW, Joshua AV, Lee JS, *Biochemistry* 21, 419–428 (1982). [PubMed: 7066293]
6. Rath CM, et al., *ACS Chem. Biol* 6, 1244–1256(2011). [PubMed: 21875091]
7. Song L-Q, Zhang Y-Y, Pu J-Y, Tang M-C, Peng C, Tang G-L, *Angew. Chem., Int. Ed* 56, 9116–9120 (2017).
8. Martinez EJ, Owa T, Schreiber SL, Corey EJ, *Proc. Natl. Acad. Sci. USA* 96, 3496–3501 (1999). [PubMed: 10097064]
9. Myers AG, Plowright AT, *J. Am. Chem. Soc* 123, 5114–5115 (2001). [PubMed: 11457349]
10. Myers AG, Lanman BA, *J. Am. Chem. Soc* 124, 12969–12971 (2002). [PubMed: 12405822]
11. Ocio EM, et al., *Blood* 113, 3781–3791 (2009). [PubMed: 19020308]
12. Carter NJ, Keam SJ, *Drugs* 70, 355–376 (2010). [PubMed: 20166769]
13. Spencer JR, et al., *Bioorg. Med. Chem. Lett* 16, 4884–4888 (2006). [PubMed: 16870445]
14. Gunaydin H, Altman MD, Ellis JM, Fuller P, Johnson SA, Lahue B, Lapointe B, *ACS Med. Chem. Lett* 9, 528–533 (2018). [PubMed: 29937977]
15. Lane JW, Chen Y, Williams RM, *J. Am. Chem. Soc* 127, 12684–12690 (2005). [PubMed: 16144418]
16. Wu Y-C, Zhu J, *Org. Lett* 11, 5558–5561 (2009). [PubMed: 19894720]
17. Liu W, Liao X, Dong W, Yan Z, Wang N, Liu Z, *Tetrahedron* 68, 2759–2764 (2012).
18. Chen R, Liu H, Chen X, *J. Nat. Prod* 76, 1789–1795 (2013). [PubMed: 24070054]
19. Saito N, Tanaka C, Koizumi Y.-i., Suwanborirux K, Amnuoypol S, Pummangura S, Kubo A, *Tetrahedron* 60, 3873–3881 (2004).
20. Xu S et al., *Eur. J. Org. Chem* 975–983 (2017).
21. Fontana A, Cavaliere P, Wahidulla S, Naik CG, Cimino G, *Tetrahedron* 56, 7305–7308 (2000).
22. Yeom H-S, Kim S, Shin S, *Synlett* 924–928 (2008).
23. Allan KM, Hong BD, Stoltz BM, *Org. Biomol. Chem* 7, 4960–4964 (2009). [PubMed: 19907787]
24. Campeau L-C, Schipper DJ, Fagnou K, *J. Am. Chem. Soc* 130, 3266–3267 (2008). [PubMed: 18293986]
25. Tan Y, Barrios-Landeros F, Hartwig JF, *J. Am. Chem. Soc* 134, 3683–3686 (2012). [PubMed: 22313324]
26. Boekelheide V, Linn WJ, *J. Am. Chem. Soc* 76, 1286–1291 (1954).
27. Wang D-S, Chen Q-A, Lu S-M, Zhou Y-G, *Chem. Rev* 112, 2557–2590 (2012). [PubMed: 22098109]
28. Lu S-M, Wang Y-Q, Han X-W, Zhou Y-G, *Angew. Chem., Int. Ed* 45, 2260–2263 (2006).
29. Shi L, Ye Z-S, Cao L-L, Guo R-N, Hu Y, Zhou Y-G, *Angew. Chem., Int. Ed* 51, 8286–8289 (2012).
30. Kita Y, Yamaji K, Higashida K, Sathaiah K, Iimuro A, Mashima K, *Angew. Chem., Int. Ed* 52, 2046–2050 (2013).
31. Wen J, Tan R, Liu S, Zhao Q, Zhang X, *Chem. Sci* 7, 3047–3051 (2016). [PubMed: 29997795]
32. Noyori R, Hashiguchi S, *Acc. Chem. Res* 30, 97–102 (1997).
33. Xie J-H, Zhu S-F, Zhou Q-L, *Chem. Rev* 111, 1713–1760 (2011). [PubMed: 21166392]
34. Dorta R, Broggini D, Stoop R, Rüegger H, Spindler F, Togni A, *Chem. Eur. J* 10, 267–278 (2004). [PubMed: 14695572]
35. *S,R**P*-BTfM-Xyliphos (**27**) is produced and sold by Solvias AG and is licensed to Sigma-Aldrich Co., and Strem Chemicals under the name SL-J008-2.
36. The lower ee measured on isolated **6** as compared to isolated **22** can be rationalized by competitive (although minor), non-selective D-ring reduction leading to the same major diastereomer. See Supplementary Materials.
37. Lavery CB, Rotta-Loria NL, McDonald R, Stradiotto M, *Adv. Synth. Catal* 335, 981–987 (2013).
38. Bruno NC, Tudge MT, Buchwald SL, *Chem. Sci* 4, 916–920 (2013). [PubMed: 23667737]
39. Pommier Y, Kohlhaagen G, Bailly C, Waring M, Mazumder A, Kohn KW, *Biochemistry* 35, 13303–13309 (1996). [PubMed: 8873596]

40. Xing C, LaPorte JR, Barbay JK, Myers AG, Proc. Natl. Acad. Sci. USA 101, 5862–5866 (2004). [PubMed: 15079082]
41. O'Brien NA, McDonald K, Luo T, Euw E, Kalous O, Conklin D, Hurvitz SA, Tomaso ED, Schnell C, Linnartz R, Finn RS, Hirawat S, Slamon DJ, Clin. Cancer Res 20, 3507–2510 (2014). [PubMed: 24879796]
42. Finn RS, Dering J, Conklin D, Kalous O, Cohen DJ, Desai AJ, Ginther C, Atefi M, Chen I, Fowst C, Los G, Slamon DJ, Breast Cancer Res. 11, R77–R89 (2009). [PubMed: 19874578]
43. Pangborn AB, Giardello MA, Grubbs RH, Rosen RK, Timmers FJ, Organometallics, 15, 1518–1520 (1996).
44. Sheldrick GM, Acta Cryst. A46, 467–473 (1990).
45. Sheldrick GM, Acta Cryst. A64, 112–122 (2008).
46. Müller P, Crystallography Reviews, 15, 57–83 (2009).
47. Comins DL, Brown JD, J. Org. Chem 49, 1078–1083 (1984).
48. Harmata M, Yang W, Barnes CL, Tetrahedron Lett. 50, 2326–2328 (2009).
49. Nicolau KC, Rhoades D, Lamani M, Pattanayak MR, Kumar SM, J. Am. Chem. Soc 138, 7532–7535 (2016). [PubMed: 27266914]
50. Tadross PM, Gilmore CD, Bugga P, Virgil SC, Stoltz BM, Org. Lett 12, 1224–1227 (2010). [PubMed: 20166704]
51. A similar compound (carbinolamine analog of jorumycin C) has been previously reported to also decompose in CDCl<sub>3</sub>, see (52).
52. Charupant K, Suwanborirux K, Amnuaypol S, Saito E, Kubo A, Saito N, Chem. Pharm. Bull 55, 81–86 (2007). [PubMed: 17202706]



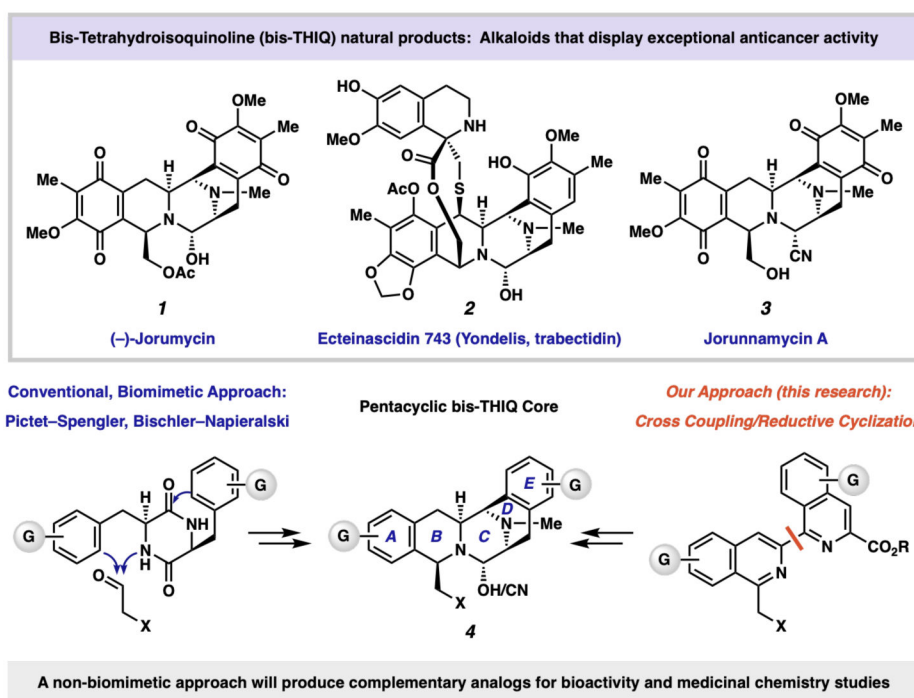


**Fig. 1. bis-Tetrahydroisoquinoline natural products.**

Jorumycin (1), ecteinascidin 743 (2), and jorunnamycin A (3). Me, methyl; Ac, acetyl; COAc, pyruvyl; X, oxygen or nitrogen substitution; G, oxygen or carbon substitution; R, generic alkyl substitution.

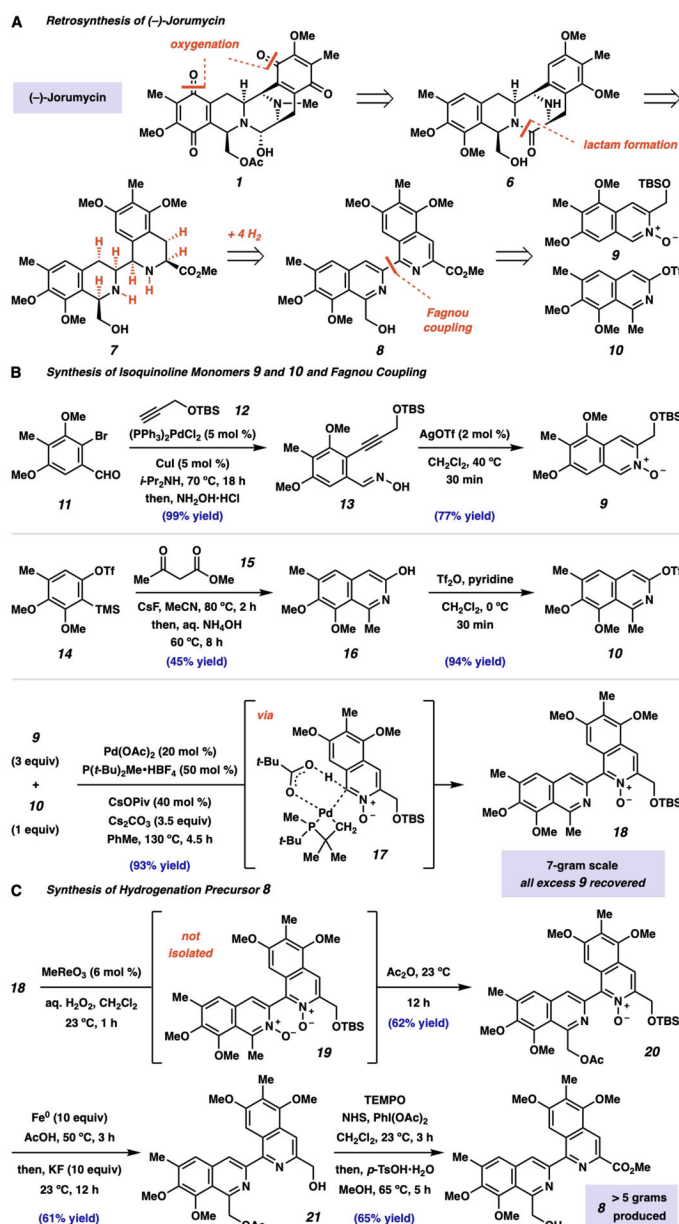


**Fig. 2. Considerations for an orthogonal synthesis of jorunnamycin A and jorumycin.** (A) Retrosynthetic analysis leading to a synthesis of jorumycin that deviates from previous synthetic strategies. (B) Isoquinoline **9** and **10** were synthesized in two steps each from aryl bromide **11** and *ortho*-silyl aryl triflate **14**, respectively. (C) Boekelheide rearrangement provided an efficient and scalable route to bis-isoquinoline **8** under mild conditions. TBS, *tert*-butyldimethylsilyl; Ph, phenyl; *i*-Pr, isopropyl; aq., aqueous; Tf, trifluoromethanesulfonyl; TMS, trimethylsilyl; MeCN, acetonitrile; *t*-Bu, *tert*-butyl; Piv, trimethyl-acetyl; equiv, molar equivalent; TEMPO, 2,2,6,6-tetramethylpiperidine-*N*-oxyl; NHS, *N*-hydroxysuccinimide; *p*-TsOH·H<sub>2</sub>O, *para*-toluenesulfonic acid monohydrate.

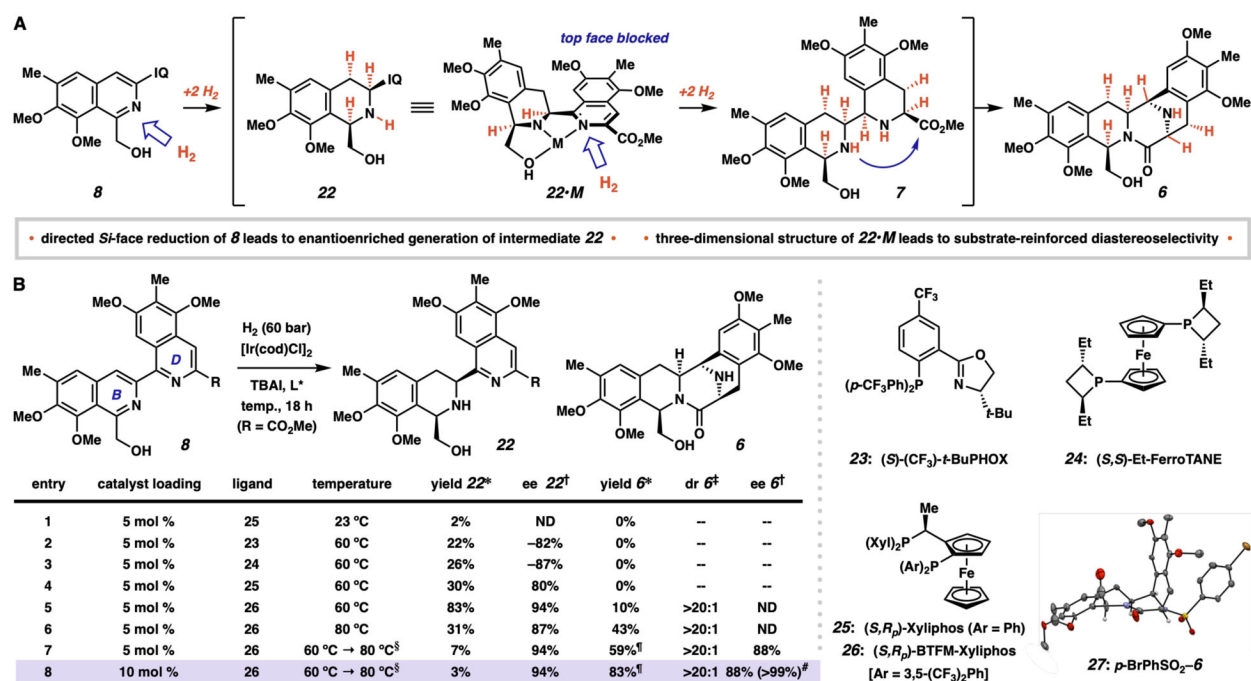


**Fig 3. Development of the enantioselective hydrogenation.**

(A) Stereochemical rationale for the enantio- and diastereoselective hydrogenation of bis-isoquinoline **8**. (B) Optimization of the hydrogenation reaction. Unless otherwise noted, all reactions were performed in 9:1 toluene:acetic acid (0.02 M) using a 1.2:1 ligand:metal ratio and a 3:1 iodide:metal ratio under a hydrogen atmosphere (60 bar) for 18 h. \*Measured by UHPLC-MS UV absorption vs. 1,3,5-trimethoxybenzene internal standard unless otherwise noted. †Measured by chiral HPLC analysis. ‡Measured by <sup>1</sup>H-NMR analysis of the crude reaction mixture. §Reaction performed at 60 °C for 18 h, then the temperature was raised to 80 °C and maintained at that temperature for 24 h. ¶Yield of isolated product after column chromatography using 10.5 mol % **26** in entry 7 and 21 mol % **26** in entry 8. #After one recrystallization. IQ, 3-carbomethoxy-5,7-dimethoxy-6-methylisoquinolin-1-yl; dr, diastereomeric ratio (major isomer vs. all others); ee, enantiomeric excess; cod, 1,5-cyclooctadiene; TBAI, tetra-*n*-butylammonium iodide; ND, not determined; Et, ethyl; Xyl, 3,5-dimethylphenyl; Ar, aryl; BTfM, 3,5-bis-trifluoromethylphenyl.

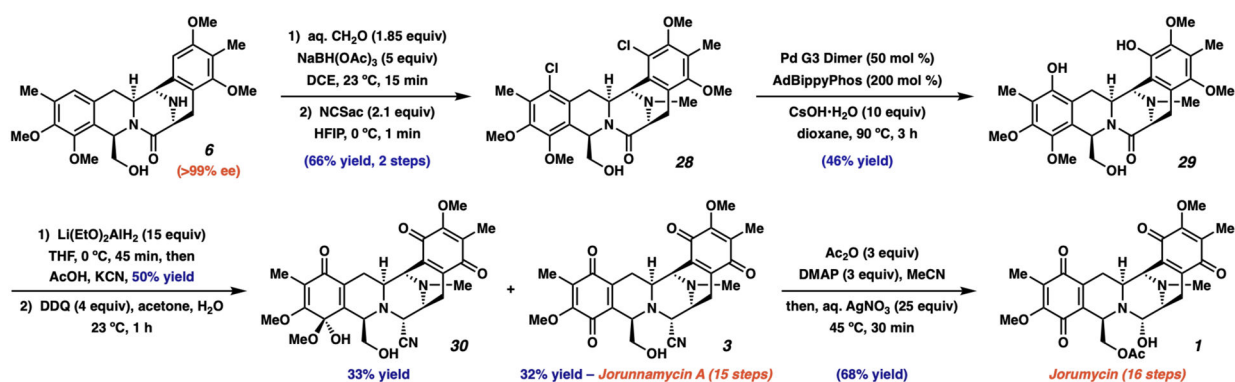
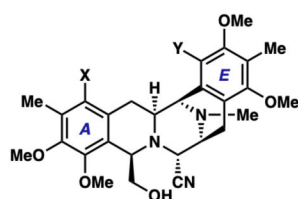


**Fig. 4. Completion of jorunnamycin A and jorumycin.**

After the reductive cyclization, five and six steps, including a palladium-catalyzed hydroxylation event, were required for the complete synthesis of jorunnamycin A (**3**) and jorumycin (**1**), respectively. DCE, 1,2-dichloroethane; NCSac, *N*-chlorosaccharine; HFIP, 1,1,1,3,3,3-hexafluoroisopropanol; Ad, 1-adamantyl; Pd G3 Dimer, (2'-Amino-1,1'-biphenyl-2-yl)methanesulfonatopalladium(II) dimer; DDQ, 2,3-dichloro-5,6-dicyano-1,4-benzoquinone; DMAP, 4-dimethylaminopyridine.



- 31:** X = Y = H → both rings partially deoxygenated  
**32:** X = OH, Y = H → E-ring partially deoxygenated  
**33:** X = H, Y = OH → A-ring partially deoxygenated  
**34:** X = Y = OH → both rings fully oxygenated

Selective, partial oxygenation allows basic SAR development

Compound	Mean IC <sub>50</sub> (nM)	Description
<b>31</b>	≥1000	full deoxygenation
<b>32</b>	708	partial (E-ring) deoxygenation
<b>33</b>	233	partial (A-ring) deoxygenation
<b>34</b>	397	full oxygenation
Carfilzomib	4	Proteasome inhibitor
Cisplatin	202	DNA binder
MK8745	360	Aurora kinase inhibitor
MMAE	438	tubulin binder

• Cytotoxicity diminished upon E-ring deoxygenation • • Cytotoxicity maintained upon A-ring deoxygenation •

### Fig. 5. Biological evaluation of non-natural analogs.

Leveraging the non-biomimetic approach to A- and E-ring construction allows for the production of previously inaccessible bis-THIQ analogs. Data reported are IC<sub>50</sub>'s measured from whole cells treated for 6 days using a 1:5 dilution series to cover a range of concentrations from 0–1 μM from an initial 10 mM DMSO stock solution of the analog in question. The IC<sub>50</sub> of each compound was calculated as a function of population doublings from baseline. MMAE, monomethyl auristatin E.